

The discovery of the multiply-imaged lensed Type Ia supernova iPTF16geu

A. Goobar,^{1*} R. Amanullah,¹ S. R. Kulkarni,² P. E. Nugent,^{3,4} J. Johansson,⁵
 C. Steidel,² D. Law,⁶ E. Mörtzell,¹ R. Quimby,^{7,8} N. Blagorodnova,²
 A. Brandeker,⁹ Y. Cao,¹⁰ A. Cooray,¹¹ R. Ferretti,¹ C. Fremling,¹² L. Hangard¹,
 M. Kasliwal,² T. Kupfer,² R. Lunnan,^{2,9} F. Masci,¹³ A. A. Miller,^{15,16}
 H. Nayyeri,¹¹ J. D. Neill,² E. O. Ofek,⁵ S. Papadogiannakis¹, T. Petrushevska¹,
 V. Ravi,² J. Sollerman,¹² M. Sullivan,¹⁴ F. Taddia,¹² R. Walters,² D. Wilson,¹¹
 L. Yan,² O. Yaron⁵

¹The Oskar Klein Centre, Physics Department, Stockholm University, Albanova University Center, SE 106 91 Stockholm, Sweden,

²Cahill Center for Astrophysics, California Institute of Technology, Pasadena, CA 91125, USA,

³Department of Astronomy, University of California, Berkeley, CA 94720-3411, USA,

⁴Lawrence Berkeley National Laboratory, 1 Cyclotron Road, MS 50B-4206, Berkeley, CA 94720, USA,

⁵Department of Particle Physics and Astrophysics, Weizmann Institute of Science, Rehovot 7610001, Israel,

⁶Space Telescope Science Institute, 3700 San Martin Drive, Baltimore, MD 21218, USA,

⁷Department of Astronomy, San Diego State University, San Diego, CA 92182, USA,

⁸Kavli IPMU (WPI), UTIAS, The University of Tokyo, Kashiwa, Chiba 277-8583, Japan,

⁹Department of Astronomy, Stockholm University, Albanova, SE 10691 Stockholm, Sweden,

¹⁰eScience Institute and Department of Astronomy, 3910 15th Ave NE Seattle, WA 98195-1570, USA,

¹¹Department of Physics & Astronomy, University of California, Irvine, CA 92697

¹²The Oskar Klein Centre, Astronomy Department, Stockholm University, Albanova University Center, SE 106 91 Stockholm, Sweden,

¹³Infrared Processing and Analysis Center, California Institute of Technology, Pasadena, CA, 91125, USA,

¹⁴Department of Physics and Astronomy, University of Southampton, Southampton, SO17 1BJ, UK,

¹⁵ Center for Interdisciplinary Exploration and Research in Astrophysics (CIERA) and Department of Physics and Astronomy, Northwestern University, 2145 Sheridan Road,

Evanston, IL 60208, USA,

¹⁶ The Adler Planetarium, 1300 S. Lakeshore Drive, Chicago, IL 60605, USA

*To whom correspondence should be addressed; E-mail: ariel@fysik.su.se.

We report the discovery of a gravitationally lensed Type Ia supernova (SN Ia) by the intermediate Palomar Transient Factory (iPTF). The light originating from SN Ia iPTF16geu, at redshift $z_{SN} = 0.409$, is magnified by an intervening galaxy at $z_l = 0.216$, acting as a gravitational lens. Using Laser Guide Star Adaptive Optics (LGSAO) OSIRIS and NIRC2 observations at the Keck telescope, as well as measurements with the Hubble Space Telescope, we were able to detect the strong bending of the light path, both for iPTF16geu and its host galaxy. We detect four images of the supernova, approximately $0.3''$ from the center of the lensing galaxy. iPTF16geu is the first SN Ia for which multiple images have been observed. From the fits of the multi-color lightcurve we derive a lensing magnification, $\Delta m = 4.37 \pm 0.15$ mag, corresponding to a total amplification of the supernova flux by a factor $\mu \sim 56$. The discovery of iPTF16geu suggests that lensing by sub-kpc structures may have been greatly underestimated. In that scenario, many discoveries of gravitationally magnified objects can be expected in forthcoming surveys of transient phenomena, opening up a new window to precision cosmology with supernovae.

One of the foundations of Einstein's theory of General Relativity is that matter curves the surrounding space. For the rare cases of nearly perfect alignment between an astronomical source, an intervening massive object, and the observer, multiple images of a single source can be seen by the observer, a phenomenon known as strong gravitational lensing.

Although many strongly lensed galaxies and quasars have been detected to date, finding this special configuration for supernovae has proved extremely difficult. The “standard candle” nature of Type Ia supernovae makes them excellent distance indicators in cosmology (1). Thus, unlike any other known source, observations of lensed SNe Ia allow us to measure the magnification provided by the lens in a model-independent way. Knowledge of absolute magnification removes the mass-sheet degeneracy (2) and the largest uncertainty in gravitational lensing measurements (3). Further, thanks to the well-known characteristics of the lightcurves, SNe Ia are ideally suited to measure time-delays in the arrival of the images, a direct probe of the expansion rate of the universe, the Hubble constant, as first shown by Refsdal (4). Time-delay measurements can also provide leverage for the studies of dark energy (5, 6). Prior to the discovery of iPTF16geu, one highly magnified SN Ia had been found in published data of the PanSTARRS1 survey (7), PS1-10afx at $z_{SN} = 1.388$ (8), with the lens later identified with redshift $z_l = 1.117$ (9). At the time of the discovery, several interpretations were discussed, including a super-luminous supernova origin. Since the lensed SN Ia hypothesis was only accepted long after the explosion had faded, no high-spatial resolution imaging could be carried out in that case. Multiple-images were resolved with the Hubble Space Telescope (HST) for SN Refsdal (10), gravitationally lensed by the large cluster of galaxies, MACS J1149.6+2223. However, that was a core-collapse SN, i.e., it could not be used to measure the lensing magnification directly.

Discovery and follow-up iPTF¹ searches the sky for new transient phenomena at optical wavelengths using image differencing between repeated observations (1), taking advantage of the large field-of-view CCD camera (7.3 sq.deg) at the 48-inch optical telescope (P48) at the Palomar Observatory (12). The first 5- σ detection of iPTF16geu (13) at RA = 21^h4^m15.86^s and

¹iPTF (2013-2016) was preceded by PTF (2009-2012).

Dec = $-6^{\circ}20'24.5''$ (J2000), near the center of the galaxy SDSS J210415.89-062024.7, is from Sep 5, 2016, although this new source was not immediately recognized by the alert software.

Spectroscopic identification was carried out with the SED Machine (*I4*) at the Palomar 60-inch telescope (P60) on Oct 2, 2016, and the object was found to be consistent with a normal SN Ia at $z \approx 0.4$, as shown in Fig. 1. For this redshift, the measured flux of the SN would be $\sim 30\text{-}\sigma$ too bright, given the normal SNe Ia brightness distribution. This led to the hypothesis that iPTF16geu could be gravitationally lensed.

Later spectroscopic observations, shown in Fig. 1, from the Palomar 200-inch telescope (P200) on Oct 4 and 6 and the Nordic Optical Telescope (NOT) on Oct 9, were used to confirm the (normal) SN Ia identification and to establish the redshift of the host galaxy from narrow Na I D absorption lines, $z_{SN} = 0.409$. The P200 and NOT spectra also show absorption features from the lensing galaxy at $z_l = 0.216$. Since then, photometric observations of iPTF16geu have been collected, both at P48 and with the SEDM Rainbow Camera (RC) at P60, which we use to estimate the peak flux, lightcurve shape and color of the SN. The measurements are needed to determine the lensing magnification, as shown in Fig. 2.

The optical observations from Palomar, with a typical seeing limited angular resolution of $2''$, are not sharp enough to spatially resolve the strong lensing nature of the system as shown in Fig. S1. To improve on that, K_s -band ($2.18 \mu\text{m}$) observations with the Natural Guide System aided Adaptive Optics (NGSAO) on the NACO instrument at the Very Large Telescope (UT1) were carried out on Oct 11, resulting in an angular resolution of $\sim 0.3''$ (FWHM) at the location of the target. From these images the first signs of structure of the system were seen, with the northeastern and southwestern parts being brighter than the center.

Multiple images of the system were first resolved on Oct 13, as seen in Fig. 3, using Laser Guide Star aided AO (LGSAO) with the OSIRIS instrument on Keck, yielding an image quality of $0.07''$ FWHM. The observation consisted of a sequence of 36 exposures of 30 s each in the

OSIRIS “ H_{bb} ” filter ($1.638 \mu\text{m}$). The resulting image reveals a partial Einstein ring with a radius of $0.27''$, together with two point sources at approximately the same radii which correspond to lensed images of the SN. The next set of LGSAO observations were carried out on Oct 20 and 21 with NIRC2, where the system was observed through the J -band ($1.1 \mu\text{m}$), besides H and K_s .

On Oct 20 and Oct 25, iPTF16geu was observed with Hubble Space Telescope. These images provide high-spatial resolution at optical wavelengths, thus extending the wavelength coverage of system. In the near-IR observations from Keck, the SN host galaxy shines brighter than at the optical wavelengths seen in the HST images in the upper panels of Fig. 3. This is expected as the SN Ia spectrum peaks at wavelengths, which after cosmological redshift, map into the F625W and F814W filters. That is the reason why two of the four SN images are not as well-resolved in the Keck images, displayed in the lower panel of Fig. 3. For the band with shortest wavelength, F475W, the effect of extinction by dust in the line of sight is also noticeable. The combined multi-wavelength observations thus provide us with an exquisite characterization of the SN images, the dimming by dust, the strongly lensed host galaxy and the lensing galaxy.

The SN Ia lightcurve Since the individual SN images cannot be resolved from the ground based observations from P48 and P60, the multi-color lightcurve in Fig. 2 represents the light from the sum of all the four SN images. The flux measurements of the SN from the RC data were derived by subtracting images from the SDSS survey (5) for each corresponding filter, since SN-free images were not available from the SEDM. This method is further described in the supplementary material.

The best fit SALT2 template (9), shown by the solid lines in Fig. 2, confirms that the observed lightcurves are fully consistent with a normal SN Ia, albeit with significantly boosted

flux. The fit also indicates a redder than average SN Ia color, suggesting that iPTF16geu suffers extinction by dust, which is further discussed in the supplementary material. This is also consistent with the observation of Na I D absorption seen in the spectra shown in Fig. 1.

The magnification can be determined by taking advantage of the fact that SNe Ia are excellent standard candles once peak brightnesses are corrected for color and lightcurve width. We use the correction parameters and the SN Ia absolute magnitude from (10) that were derived from 740 SNe Ia using the same SALT2 lightcurve fitter, and find a magnification of 4.37 ± 0.15 mag, where the brightness dispersion of normal SNe Ia has been taken into account. This corresponds to an amplification $\mu \approx 56$ of the SN flux. Note that this measurement is independent of the value of the Hubble constant or any other cosmological parameter, since we are comparing the brightness of this SN to other SNe Ia at the same redshift.

The resolved lensed system The system shown in Fig. 3 exhibits multiple images originating from both iPTF16geu and the SN host galaxy at an angular scale $0.26''$ – $0.31''$.

A “ring-like” structure originating from the extended host galaxy, as well as four SN images are detected, with nearly 90° azimuthal separations. The system is consistent with the lens being described by an isothermal ellipsoid galaxy (18, 19) with a velocity dispersion of $\sigma_v \sim 140 \text{ km s}^{-1}$ (or in the case of the dynamics being dominated by rotational motion, a rotational velocity of $v_c \sim 200 \text{ km s}^{-1}$), corresponding to a mass of $M \sim 1.4 \times 10^{10} M_\odot$ within a radius of 0.9 kpc. The data is compatible with a moderate ellipticity of the lensing galaxy and a small or zero core radius. This is possibly the first time that galaxy mass structure on sub-kpc scales has been resolved through strong lensing, with the exception of microlensing events. None of the 299 systems in the Master Lens Database², where the redshifts of the source and lens galaxy are known, probe scales below 1 kpc.

²<http://admin.masterlens.org>

The velocity dispersion in the lens model is compatible with the measured width of the spectral lines for the lensing galaxy shown in Fig. 1, assuming that is dominated by Doppler broadening. The lens model suggests time-delays between the four SN images up to 100 hours. Accurate measurements of these will be challenging, and require observations of the system also after the SN has faded (in about one year), to allow for a subtraction of the galaxy light contamination, both from the host and lens, needed to isolate the SN flux in each one of the SN images.

Summary and outlook SNe Ia are unique tools to discover lensing by small structures since the systems can be identified, even without the need of high spatial resolution. These systems would be otherwise very hard to find, if not impossible. With iPTF16geu, we have established the feasibility to discover strongly lensed “standard candles” live, even with a modest telescope at a less than optimal site. We were then able to trigger multi-wavelength follow-up observations from space and AO facilities, which will allow us to accurately measure the SN image positions and flux ratios, as well as constrain the time-delay between the multiple images. The observations serve also to carefully study the lensed SN host galaxy and the lensing galaxy.

For iPTF16geu, we expect to measure the difference in arrival time between the SN images with an accuracy of ~ 2 hours, which under favorable conditions would lead to an estimate of H_0 with 2% precision, i.e., comparable to the best local estimates to date (20), which are in tension with the global estimate of the expansion rate measured by the Planck mission (21).

The iPTF discovery of this seemingly rare event raises intriguing questions about the rates of strongly lensed SNe Ia. To date, almost 2000 SNe Ia up to $z \sim 0.2$ have been discovered and classified within the PTF and iPTF surveys over a period of eight years (945 observing nights), with a detection limit of $R \sim 21$ mag. Since they are brighter, lensed SNe can be observed to higher redshifts. We estimate that within the larger volume up to $z = 0.4$, the number of SNe Ia

explosions is $12.6 \text{ sq.deg}^{-1} \text{ year}^{-1}$, which when combined with the total monitoring time and the average solid angle of the survey, yields a total of 6×10^4 SNe Ia in the field of view, and a relative fraction 1.7×10^{-5} for events like iPTF16geu, if this single event is representative of the rate³.

We have simulated 10^7 lines of sight with the redshift distribution probed by iPTF using the SNOC Monte-Carlo package (22) which suggests that finding a lensed SNe Ia with $\mu \geq 50$ within our eight year survey has a probability of up to 7%, in the most optimistic scenario. However, to get to even to the few percent level, extreme assumptions have to be made, e.g., about the fraction of compact objects in galaxy halos. The same code has been used in the past to accurately describe the weak lensing magnification of high-redshift SNe Ia (23).

Thus, either iPTF16geu was a rather unlikely event, or, as suggested by the fact that PS1-10afx also had a very high lensing magnification, the actual rate of strongly lensed SNe is more favorable than anticipated. The latter case would have implications for our understanding of how dark matter is clumped. We also note that strong gravitational lensing has been proposed as a powerful tool to explore theories of gravity beyond General Relativity (24). Thus, the discovery of Type Ia SN iPTF16geu, strongly magnified by an unusually small lens, likely opens a new window into precision studies of gravity and cosmology.

If the rate of strongly lensed SNe Ia is well-described by the occurrence of this single event, it bodes well for the prospects of detecting many such systems with the forthcoming Zwicky Transient Facility (ZTF, more than ten times faster than iPTF), to start regular observations in August 2017. By 2020, the Large Synoptic Survey Telescope (LSST) and around 2025 the WFIRST satellite will reach much higher redshifts, dramatically enlarging the volume that can be probed, potentially leading to a large number of strongly lensed SN Ia discoveries in the near future. This would likely have transformational implications for our means to measure the

³In this calculation we have corrected for the average efficiency in transient detection and spectroscopic typing over the lifetime of the survey.

Hubble constant, for the study of galaxy sub-structures, and possibly for tests of theories of modified gravity.

References and Notes

1. A. Goobar, B. Leibundgut, *Annual Review of Nuclear and Particle Science* **61**, 251 (2011).
2. E. E. Falco, M. V. Gorenstein, I. I. Shapiro, *ApJL* **289**, L1 (1985).
3. P. Schneider, D. Sluse, *A&A* **559**, A37 (2013).
4. S. Refsdal, *MNRAS* **128**, 307 (1964).
5. A. Goobar, E. Mörtzell, R. Amanullah, P. Nugent, *A&A* **393**, 25 (2002).
6. S. H. Suyu, *et al.*, *ApJ* **766**, 70 (2013).
7. R. Chornock, *et al.*, *ApJ* **767**, 162 (2013).
8. R. M. Quimby, *et al.*, *ApJL* **768**, L20 (2013).
9. R. M. Quimby, *et al.*, *Science* **344**, 396 (2014).
10. P. L. Kelly, *et al.*, *Science* **347**, 1123 (2015).
11. Y. Cao, P. E. Nugent, M. M. Kasliwal, *PASP* **128**, 114502 (2016).
12. N. M. Law, *et al.*, *PASP* **121**, 1395 (2009).
13. A. Goobar, *The Astronomer's Telegram* **9603**, 1 (2016).
14. A. Ritter, C. C. Ngeow, N. Konidakis, R. Quimby, S. Ben-Ami, *Contributions of the Astronomical Observatory Skalnaté Pleso* **43**, 209 (2014).

15. S. Alam, *et al.*, *ApJS* **219**, 12 (2015).
16. J. Guy, *et al.*, *Astronomy and Astrophysics* **466**, 11 (2007).
17. M. Betoule, *et al.*, *Astronomy and Astrophysics* **568**, A22 (2014).
18. A. Kassiola, I. Kovner, *Liege International Astrophysical Colloquia*, J. Surdej, D. Fraipont-Caro, E. Gosset, S. Refsdal, M. Remy, eds. (1993), vol. 31 of *Liege International Astrophysical Colloquia*, p. 571.
19. R. Kormann, P. Schneider, M. Bartelmann, *A&A* **284**, 285 (1994).
20. A. G. Riess, *et al.*, *ApJ* **826**, 56 (2016).
21. Planck Collaboration, *et al.*, *A&A* **571**, A16 (2014).
22. A. Goobar, *et al.*, *A&A* **392**, 757 (2002).
23. J. Jönsson, *et al.*, *ApJ* **639**, 991 (2006).
24. K. Koyama, J. Sakstein, *PRD* **91**, 124066 (2015).
25. AG and RA acknowledge support from the Swedish National Science Council (VR) and the Swedish Space Board. The iPTF Swedish collaboration is funded through a grant from the Wallenberg foundation. We are grateful for support from the National Science Foundation through the PIRE GROWTH project, Grant No 1545949.

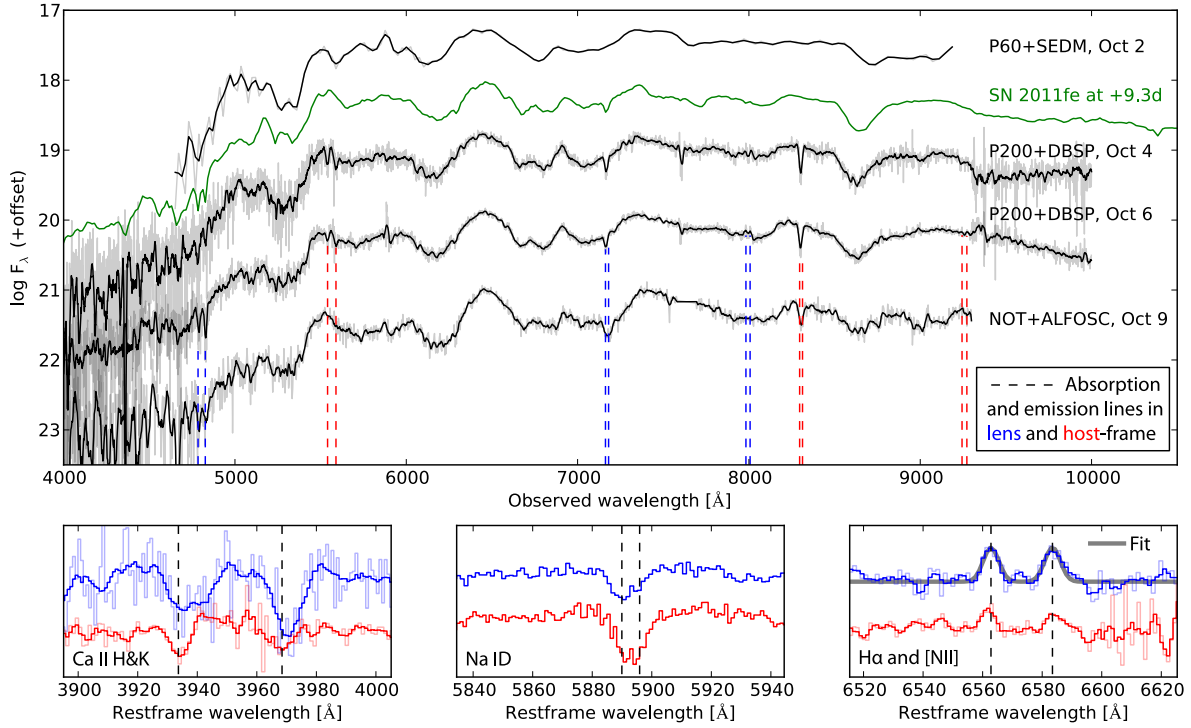


Figure 1: Spectroscopy of iPTF16geu obtained with P60, P200 and NOT telescopes. All spectra are best fit with a normal SN Ia at the corresponding epochs, as shown by the comparison of the best ever studied near-by SN Ia, SN 2011fe (green line, with data from 18). The spectra also reveal narrow absorption and emission lines, marked by the dashed vertical lines, from which the redshifts of the lens ($z_l = 0.216$, blue lines) and SN host galaxy ($z_{SN} = 0.409$, red lines) were determined. A zoomed in view, in rest-frame wavelengths, of the Ca II H & K and Na ID absorption features (left and middle bottom panels, respectively) together with the H_α and [N II] emission lines are shown in the bottom left, middle and right panels, respectively. In particular, the H_α and [N II] emission lines at $z_l = 0.216$ allows us to fit for the velocity dispersion of the lensing galaxy (see Supplementary material for details).

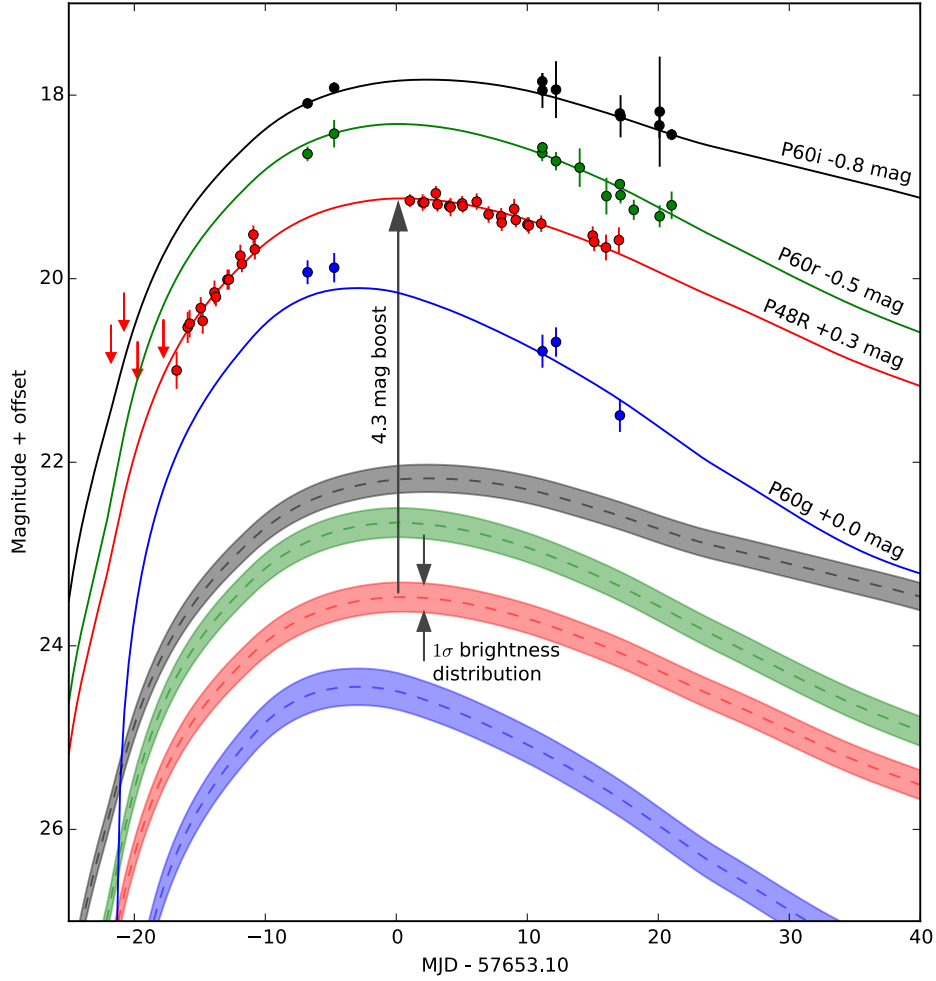


Figure 2: Lightcurve for iPTF16geu the *R*-Mould band from P48, and *gri* from RC on the SEDM at P60. The solid lines show the best fitted SALT2 (9) model to data. The dashed lines show the expected lightcurves at $z = 0.409$ where the bands represent the standard deviation of the brightness distribution for SNe Ia. In order to fit the observed lightcurves a brightness boost of 4.3 magnitudes is required.

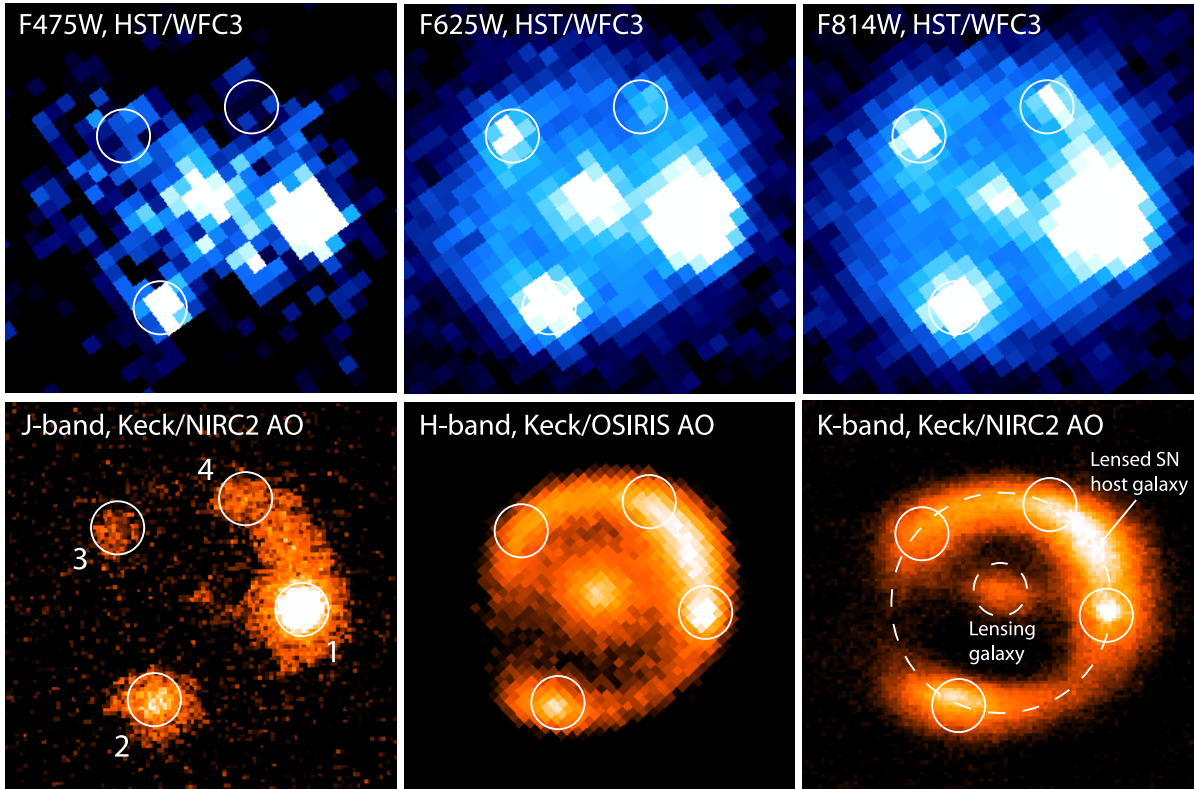


Figure 3: *Top panel:* HST/WFC3 observations of iPTF16geu obtained on Oct 25 2016 in the F475W, F625W and F814W bands. The images clearly reveals four point sources in all bands except for F475W where images 3 and 4 are not visible. *Bottom panel:* NIR images obtained using Adaptive Optics aided Keck observations in the J , H and K_s bands. The H band was obtained on Oct 13 while K_s and J bands were obtained on Oct 22–23. For the H and K_s images, both the lensing galaxy at the center of the system and the lensed Einstein ring of the host galaxy are clearly visible. The details of the observations are described in the supplementary material. The sizes of the patches are $1'' \times 1''$ where North is up and East is left.

Supplementary material

1 Discovery and observations

1.1 P48 survey and P60 follow-up

Since late August 2016, the intermediate Palomar Transient Factory has been performing a mixed-cadence experiment. About 100 fields ($\simeq 700$ square degrees in sky area) are observed every night, while another 200 fields are observed every three nights. During a night, each field is visited twice separated by an hour. For fields with available SDSS g - and Mould R -band reference images, these two visits are one in each filter. For fields with only R -band reference images, these two visits are both in the R -band.

Images are transferred and processed by our real-time image subtraction pipeline at the National Energy Research Scientific Computing Center (1). This pipeline, equipped with high-performance computing and machine-learning transient classifiers (2, 3), delivers transient candidates for visual inspection by our duty astronomers within ten minutes of images being taken.

On Sep 11, our duty astronomer identified a transient candidate near the core of the galaxy SDSS J210415.89-062024.7 in one R -band-only one-day cadence field. This candidate was saved as iPTF16geu (a.k.a. AT2016geu) and put in the queue for spectroscopic classification. However, iPTF16geu was not observed spectroscopically until Oct 2, as described below, and both the redshift and the transient type was unknown until that point.

Meanwhile the field was observed with a daily cadence in the R -band. Difference imaging photometry in Mould R -band was obtained using the IPAC/iPTF Discovery Engine (4, IDE), where reference images are aligned and matched to have the same point spread function (PSF) to the images where the SN is active. An example of aligned and PSF matched images is shown in the top panel of Fig. S1. PSF photometry is then carried out and calibrated by matching the

photometry of the field stars to the stellar catalog from the Sloan Digital Sky Survey (5, *SDSS*).

Complementary follow-up photometry was obtained in the $g'r'i'$ -bands with the Rainbow Camera (RC) on the the Spectral Energy Distribution Machine (SEDM) mounted on the Palomar 60-inch telescope (P60). For the redshift of iPTF16geu, $z_{SN} = 0.409$, these filters provide an excellent match to the restframe UBV filters as shown in Fig. S2 that historically have been used for studying SNe Ia. SEDM is a Caltech-developed instrument, designed for fast transient classification and follow-up. The SEDM focal plane combines a photometric instrument, the RC, and an Integral Field Unit (IFU) spectrograph. The focal plane of the RC is split into four quadrants, each one containing a Sloan generation 2 filter: $u'g'r'i'$. The FoV is 6.5 arcmin^2 for each filter. The IFU, designed as a lenslet array, is mounted in the center. Its FoV is 30 arcsec^2 and each spaxel covers an approximate diameter of $0.7''$. The instrument covers the optical range $4000\text{--}9500 \text{ \AA}$ with a constant resolution of $R \simeq 100$, equivalent to 3000 km s^{-1} .

The RC data was pre-processed following standard photometry reduction techniques. The host subtraction was done by using the automatic reference-subtraction photometry pipeline `FPipe` (6). This is using a similar approach to IDE, but images from the Sloan Digital Sky Survey are used as reference images of the host galaxy since such data is not available from the RC. The photometric uncertainty is determined as the measured scatter from placing artificial PSFs in a circular pattern around the real transient and measuring their values on the subtracted images.

The first classification spectrum of iPTF16geu was obtained with the IFU on the SEDM on Oct 2 2016. The combined spectrum shown, in Fig. 1 in the main paper, consists of the average of two 1350 s exposures, taken at an initial airmass of 1.4 and an average FWHM of $1.65''$ and $S/N \sim 15$. The offset of $10''$ between the exposures has allowed the subtraction of the skylines. The data was reduced using a custom IFU pipeline developed for the instrument (7). Flux calibration and correction of telluric bands were done using the standard star BD+28d4211,

which was taken at a similar airmass. An aperture of $4''$ was used to extract the spaxels.

1.2 Additional spectroscopic follow-up

The classification and redshift of iPTF16geu from the low-resolution SEDM IFU spectrum was confirmed by observations obtained with the Double Spectrograph (8, *DBSP*) mounted on the Palomar 200-inch telescope (P200) on Oct 3 and Oct 6, and using the ALFOSC instrument on the Nordic Optical Telescope (NOT) on Oct 9.

For the DBSP observations the 600/4000 grating was used with slitwidths $1.5''$ and $2''$ and exposure times 900 s and 870 s, respectively. The observations were taken at airmass 1.370 and 1.476 and reduced with a custom pipeline based on PyRAF. Flux calibration and telluric correction were done with flux standard stars. The spectra cover the wavelength ranging from 3200 \AA to $10\,300 \text{ \AA}$.

For the ALFOSC spectrum grism #4 was used with the slitwidth $1.0''$ and exposure time 2700 s. The observation was taken at airmass 1.224 and the data were reduced with a custom pipeline written in Matlab. Wavelength calibration was performed with a He-Ne arc lamp, and flux calibration with a standard star observed the same night at similar airmass. The full spectrum covers the range 3557 \AA and 9711 \AA .

1.3 Adaptive Optics observations of iPTF16geu

1.3.1 NGS AO image from VLT

K_s -band ($2.18 \mu\text{m}$) observations were obtained on Oct 11 2016 using NAOS-CONICA (NACO) at the Very Large Telescope (VLT). The bright star with $V = 11.5 \text{ mag}$ $29.5''$ SE of iPTF16geu, seen in the upper panel of Fig. S1, was used as a natural guide star (NGS). Due to problems with the visual wave-front sensor, the IR wavefront sensor with the N20C80 dichroic was used. The observations were made with a standard jitter pattern in a $5''$ box with single exposure

integrations of 20 s, saved in cube mode. In total, 348 frames were obtained. We reduced the data with the NACO `esorex` pipeline, using the standard jitter recipe. Since all exposures were individually saved, we attempted to improve the resolution by selecting the best-resolved 20 % of the frames, with small improvement. The resulting image, shown in the lower panel of Fig. S1, has an image quality of $\text{FWHM} \sim 0.3''$ at the location of the target, with a Strehl ratio of $\sim 5\%$.

1.3.2 LGS AO image from Keck

LGS AO image from Keck iPTF16geu was observed with the OSIRIS imager behind the Keck I laser guide star adaptive optics (LGS AO) system on Oct 13 2016 and separately with the Keck II NIRC2 near infrared imager in the J , H and K_s bands (at $1.2 \mu\text{m}$, $1.6 \mu\text{m}$ and $2.2 \mu\text{m}$ respectively) on Oct 22 and 23 2016. The field of view of the OSIRIS imager is 20 square arcsec and is sampled with $0.02''$ pixels by a 1024×1024 Hawaii 1 HgCdTe array. The observation consisted of a sequence of 36 exposures of 30 s each in the OSIRIS “ H_{bb} ” filter ($1.638/0.330 \mu\text{m}$), dithered in a 3×3 box pattern with $2.5''$ separation. The NGS SE of iPTF16geu mentioned above was used as the tip/tilt star. Immediately following the iPTF16geu observation, the tip/tilt star field was centered on the OSIRIS imager and a short sequence of dithered observations was taken as a PSF reference, yielding point source $\text{FWHM} \simeq 0.07''$ (as measured from an $H = 15$ mag star near the bright tip/tilt star).

The OSIRIS data were reduced using standard infrared self-calibration techniques. First, the 36 individual frames were scaled to a common median and combined into a super-sky frame using a $3\text{-}\sigma$ clipped mean algorithm, masking out a $2'' \times 2''$ box around the location of the target source in each frame. This super-sky was divided by its own median in order to produce a super-flat image that was then used to flatfield the individual science frames. The median unmasked value was then subtracted from each flatfielded science frame in order to produce the flatfielded,

foreground-subtracted science frames. These frames were then shifted by the header-derived dither offsets (adjusted slightly by hand to ensure proper alignment) and combined using a $3\text{-}\sigma$ clipped mean algorithm. The final image is shown in Fig. S1.

The NIRC2 observations consist of 39 exposures of 80 s each in the K_s band and 9 and 6 exposures of 120 s each in the H and J bands respectively. We used the same tip-tilt star as OSIRIS observations for the AO corrections. The observations were carried out using the NIRC2 narrow camera with a field of view of 100 square arcsec and a pixel scale of $0.01''/\text{pixel}$. We dithered each of the frames by $2''$ using a custom nine-point dithering pattern for better sky subtraction. To correct for flat-fielding and dark currents we acquired a set of ten dark frames and twenty dome flat frames. The dome flats were separated into two sets with the first half in dome flat off and second half in dome flat on configurations. The individual dark and flat frames were combined to generate master dark and dome flat frame respectively. The observations were processed using custom IDL routines to combine the individual frames in each bands. This produced a combined dark and flat subtracted image in the J , H and K_s bands.

1.4 WFC3/HST observations

The HST WFC3 images presented in Fig. 3 in the main paper were obtained under program DD 14862 (PI: Goobar) using the UVIS channel on Oct 25 2016 in the F475W, F625W and F814W filters (where the filter names correspond to the central wavelengths in nm). UVIS consists of two e2V thinned, backside illuminated, UV optimized 2048×4096 CCDs. However, only part of the UVIS2 chip was read for the iPTF16geu observations using the UVIS2-C512C-SUB aperture. UVIS has a pixel scale of $0.04''/\text{pixel}$ and the diffraction limited PSF for these filters results in an image quality of $\text{FWHM} \simeq 0.07''$. We used a standard 3-point dithering pattern with post-flash to maximize the charge transfer efficiency (CTE) during read-out. The total exposure time for the three filters were 378 s, 291 s and 312 s for F475W, F625W and F814W,

respectively.

The images were automatically processed through the `calwf3` pipeline where they are dark subtracted, flat fielded and CTE-corrected. Further, the individual flatfielded images were combined and corrected for geometric distortion using the STScI `AstroDrizzle` software.

2 Fitting to a SN Ia lightcurve template

The lightcurves from the P48 and P60 photometry are shown in Figs. 1, in the main paper, and in S3. Since SNe Ia is a homogenous class of objects, templates or lightcurve models can typically be fitted to the data. The free parameters are the time, t_0 , and brightness, m_B^* , of maximum in the rest-frame B -band, the lightcurve width and the color of the SN.

The lightcurve width can be quantified by introducing a stretch factor, s , that scales the time variable of the template with respect to t_0 . The same behavior is also captured by the first principal component of the SALT2 lightcurve model (9). This component is describing the diversity from the the average SN Ia spectral sequence. Both are obtained from training the model on a large data set of normal SNe Ia. The eigenvalue for the first component, x_1 , is normalized so that a SN with $x_1 = 0$ has an average lightcurve width, while $x_1 = \pm 1$ corresponds to one standard deviation in the distribution of normal SNe Ia lightcurve widths.

The color is typically defined in terms of the restframe $B - V$ magnitude. This is then used to scale a color, or extinction, law that describes how the flux ratios vary with wavelength. For a standard extinction law, the color excess, $E(B - V)$, is used to scale the law, where $E(B - V)$ is the $B - V$ magnitude deviation from what would have been measured in the absence of extinction. SALT2 is using an empirically derived color law where the scaling parameter, \mathcal{C} , is the deviation from the average $B - V$ restframe color.

In this work we fitted both a lightcurve template and the SALT2 model to the P48 and P60 photometry. In Fig. 1 in the main paper we show the best fitted SALT2 model which is the same

model used for the SN Ia cosmology sample presented in (10). Using the same model allows us to estimate the magnification independently of the value of H_0 , or any other cosmological parameter. The SALT2 model has four free parameters, for which we obtain, $t_0 = 57654.1 \pm 0.2$, $m_B^* = 19.12 \pm 0.03$, and $\mathcal{C} = 0.23 \pm 0.03$ and $x_1 = 0.08 \pm 0.19$, respectively. The corrected peak magnitude, m_B^{corr} , is further obtained as

$$m_B^{\text{corr}} = m_B^* - \beta \cdot \mathcal{C} + \alpha \cdot x_1$$

where $\beta = 3.101 \pm 0.075$ and $\alpha = 0.141 \pm 0.006$ derived for the the full sample in (10) were used. The expected lightcurves, adopting the results from (10), for the source redshift is shown in Fig. 2 in the main paper, together with the intrinsic dispersion. When we compare the derived peak magnitude with the expected, we find that the SN has been boosted by 4.30 ± 0.15 magnitudes where the intrinsic dispersion is accounted for in the quoted error bar.

We also tried to fit the spectral series of SN 2011fe, which is a normal and well observed SN Ia, to the data. In Fig. S3 we show both the SALT2 lightcurve model and the best SN 2011fe fit using the spectral series for the latter compiled by (11). We note that the data are perfectly consistent with both models but that SN 2011fe provides a better fit in the restframe U -band. iPTF16geu has the same lightcurve shape as SN2011fe, but a reddening of $E(B - V) = 0.31 \pm 0.05$ is required, assuming an extinction law from (12) with $R_V = 3.1$.

Both the SALT2 model and SN 2011fe fits show that the iPTF16geu is perfectly consistent with a normal and average SNe Ia, but the derived values of \mathcal{C} and $E(B - V)$ suggest that that the SN could be reddened. For the lightcurve fits presented here, it has been assumed that any reddening, if present, happens in the host galaxy of the SN, but it is quite possible that iPTF16geu also could be reddened by the lensing galaxy. We have measured the flux ratios between the F814W and F625W filters in the HST/WFC3 data for the two brightest images and find that they are consistent with each other. Since these are the two brightest images, and they

take different paths through the lensing galaxy this, this measurement suggests that the majority of the light is not affected by the lensing galaxy.

References and Notes

1. Y. Cao, P. E. Nugent, M. M. Kasliwal, *PASP* **128**, 114502 (2016).
2. H. Brink, *et al.*, *MNRAS* **435**, 1047 (2013).
3. U. Rebbapragada, B. Bue, P. R. Wozniak, *American Astronomical Society Meeting Abstracts* (2015), vol. 225 of *American Astronomical Society Meeting Abstracts*, p. 434.02.
4. F. Masci, *et al.*, *ArXiv e-prints* (2016).
5. S. Alam, *et al.*, *ApJS* **219**, 12 (2015).
6. C. Fremling, *et al.*, *A&A* **593**, A68 (2016).
7. Blagorodnova, *et al.*, in prep.
8. J. B. Oke, J. E. Gunn, *PASP* **94**, 586 (1982).
9. J. Guy, *et al.*, *Astronomy and Astrophysics* **466**, 11 (2007).
10. M. Betoule, *et al.*, *Astronomy and Astrophysics* **568**, A22 (2014).
11. R. Amanullah, *et al.*, *Monthly Notices of the Royal Astronomical Society* **453**, 3300 (2015).
12. J. A. Cardelli, G. C. Clayton, J. S. Mathis, *ApJ* **345**, 245 (1989).

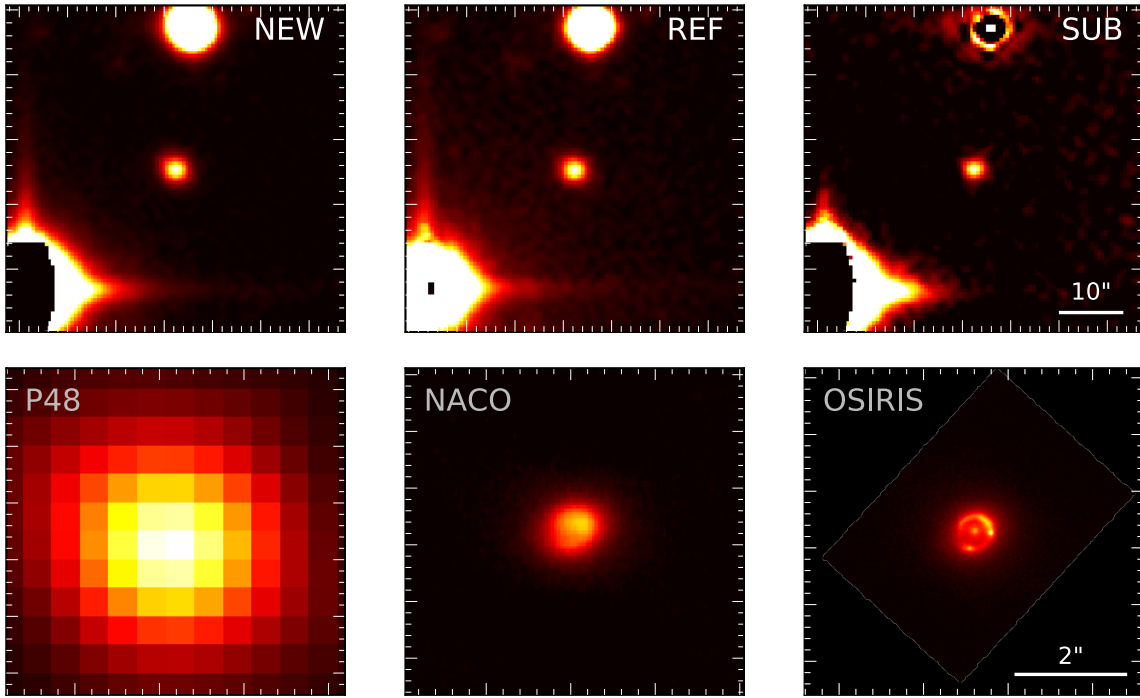


Figure 4: *Top panels:* P48 *R*-band images of SDSS J210415.89-062024.7, where the first image includes the SN, the second is the host galaxy reference image made of pre-explosion images, and the last is the subtraction between the two. The last frame shows that the bright and saturated stars do not subtract perfectly which is normal. The brightness excesses due to this will be discarded by the machine learning algorithm and will not be confused as astronomical transients. The brightness excess shown in the centre is iPTF16geu. *Bottom panels:* Comparison in image quality between P48 (shown in the top panel) the NGS AO NACO image from VLT and the best resolution AO LGS image from Keck.

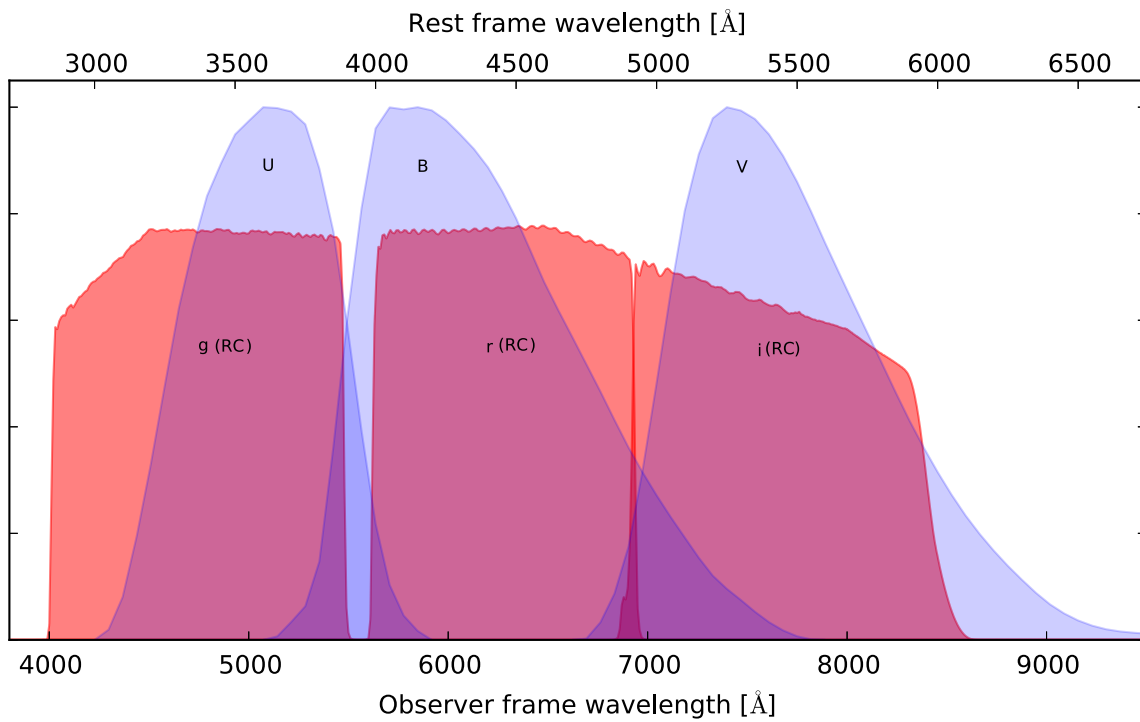


Figure 5: Comparison between the P60 RC filters, shown in the red, used in this work with the standard rest-frame (as indicated by the upper horizontal axis) UBV filters which historically have been used for studying SNe Ia. It is clear from the figure that the observer frame RC $g'r'i'$ filters provide a close match to the rest-frame UBV for the given redshift $z_{SN} = 0.409$.

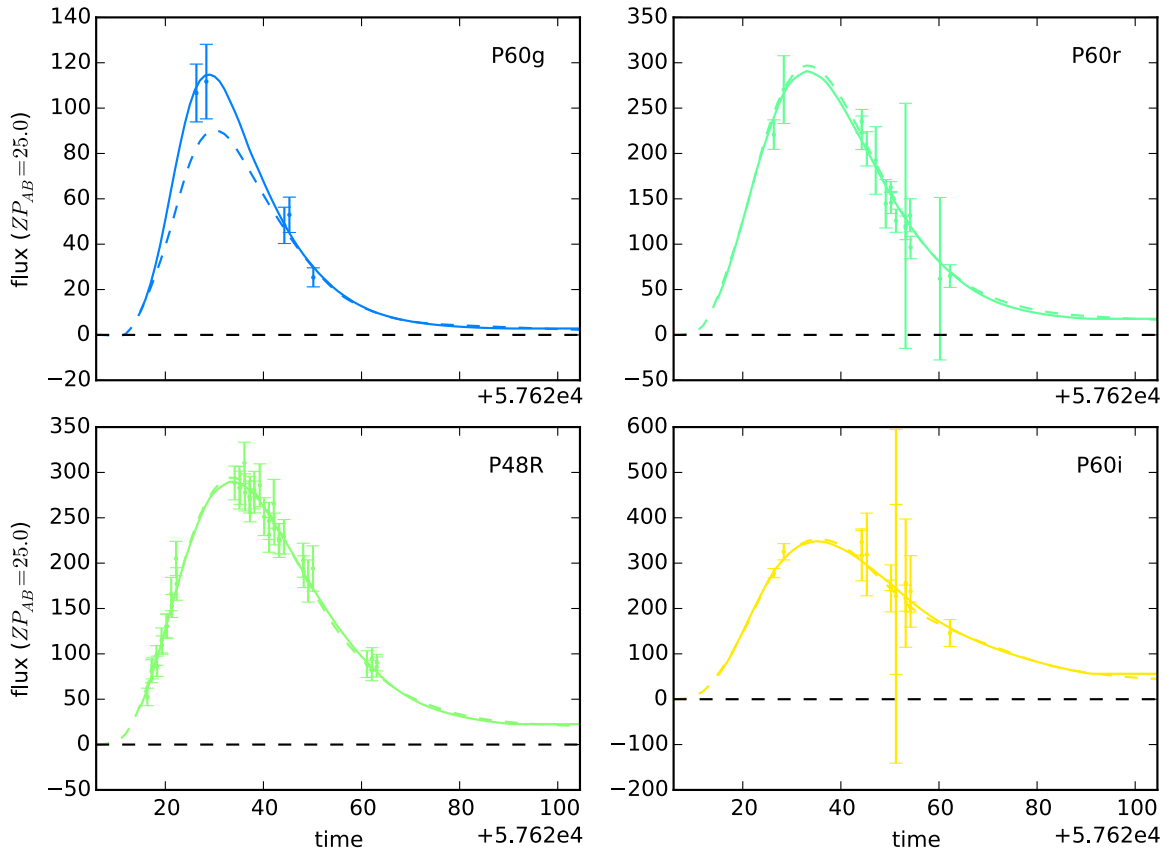


Figure 6: Lightcurves of iPTF16geu in the P48 R -band and the P60 RC $g'r'i'$ bands. The error bars are correlated. The solid lines show the fit of the nearby and normal SN 2011fe, while the dashed show the best fit using the SALT2 model.